Spatial and temporal mapping of the PfEMP1 export pathway in *Plasmodium falciparum*

Paul J. McMillan[1,2,3], **Coralie Millet**[#,1,2,3], **Steven Batinovic**[#,1,2,3], **Mauro Maiorca**[1,2,3], **Eric Hanssen**[2,3,4], **Shannon Kenny**[1,2,3], **Rebecca A. Muhle**[5], **Martin Melcher**[6], **David A. Fidock**[7], **Joseph D. Smith**[6], **Matthew W.A. Dixon**[1,2,3], and **Leann Tilley**[*,1,2,3]

[1]Department of Biochemistry and Molecular Biology, The University of Melbourne, Melbourne, VIC 3010, Australia

[2]ARC Centre of Excellence for Coherent X-ray Science, The University of Melbourne, Melbourne, VIC 3010, Australia

[3]Bio21 Molecular Science and Biotechnology Institute, The University of Melbourne, Melbourne, VIC 3010, Australia

[4]Advanced Microscopy Facility, The University of Melbourne, Melbourne, VIC 3010, Australia

[5]Department of Microbiology & Immunology, Albert Einstein College of Medicine of Yeshiva University, Bronx, NY 10461, USA

[6]Seattle Biomedical Research Institute, Seattle, WA 98109, USA

[7]Department of Microbiology & Immunology, Columbia University Medical Center, New York, NY 10032, USA

Summary

The human malaria parasite, *Plasmodium falciparum*, modifies the red blood cells (RBCs) that it infects by exporting proteins to the host cell. One key virulence protein, *P. falciparum* Erythrocyte Membrane Protein-1 (PfEMP1), is trafficked to the surface of the infected RBC, where it mediates adhesion to the vascular endothelium. We have investigated the organization and development of the exomembrane system that is used for PfEMP1 trafficking. Maurer's cleft cisternae are formed early after invasion and proteins are delivered to these (initially mobile) structures in a temporally staggered and spatially segregated manner. Membrane-Associated Histidine-Rich Protein-2 (MAHRP2)-containing tether-like structures are generated as early as 4 h post-invasion and become attached to Maurer's clefts. The tether/ Maurer's cleft complex docks onto the RBC membrane at ~20 h post-invasion via a process that is not affected by cytochalasin D treatment. We have examined the trafficking of a GFP chimera of PfEMP1 expressed in transfected parasites. PfEMP1B-GFP accumulates near the parasite surface, within membranous structures exhibiting a defined ultrastructure, before being transferred to pre-formed mobile Maurer's clefts. Endogenous PfEMP1 and PfEMP1B-GFP are associated with Electron-Dense Vesicles that may be responsible for trafficking PfEMP1 from the Maurer's clefts to the RBC membrane.

---

[*]To whom correspondence should be addressed: Professor Leann Tilley, Department of Biochemistry and Molecular Biology, Bio21 Molecular Science and Biotechnology Institute, 30 Flemington Road, The University of Melbourne, Melbourne, Victoria 3010, Australia, Phone: 61-3-8344-2227, Fax: 61-3-9348-1421, ltilley@unimelb.edu.au.
[#]These authors contributed equally

Introduction

Malaria is responsible for a huge annual death toll - estimated to be from 640,00 (World Health Organisation, 2011) to more than 1.2 million (Murray *et al.*, 2012) - mostly caused by *Plasmodium falciparum*. The deaths result from complications of malaria that arise during the blood stages of the infection (Rowe *et al.*, 2009, Fairhurst *et al.*, 2012). In this phase *P. falciparum* develops inside red blood cells (RBCs) and alters their surface properties resulting in adhesion to endothelial cells, rosetting with uninfected RBCs and platelet-mediated clumping (McPherson *et al.*, 1985, Carlson *et al.*, 1990, Roberts *et al.*, 1992).

Cytoadhesion contributes to the virulence of *P. falciparum* by preventing the clearance of infected RBCs by the spleen, thereby permitting a more rapid multiplication rate (Langreth *et al.*, 1985). The sequestered mass of infected RBCs can lead to microvascular obstruction (Dondorp *et al.*, 2004) and metabolic disturbances, such as acidosis (Planche *et al.*, 2006). Moreover, an inappropriate host immune response to the sequestered parasites can precipitate complications that lead to coma and death (Turner *et al.*, 1994, Hansen *et al.*, 2010, Kim *et al.*, 2011, Grau *et al.*, 2012). While total malaria infections are decreasing the incidence of severe malaria is increasing in some endemic areas, possibly due to intervention measures that decrease the general level of immunity (Okiro *et al.*, 2011, Eastman *et al.*, 2009).

Adhesion of infected RBCs is mediated by a multi-protein complex that the parasite traffics to and assembles at the RBC membrane (Scherf *et al.*, 2008, Baruch *et al.*, 1995). A critical component of the virulence complex is the *P. falciparum* Erythrocyte Membrane Protein-1 (PfEMP1), which is inserted into the RBC membrane at raised platforms known as knobs. PfEMP1 is anchored to the knob complex via its C-terminal cytoplasmic domain, also known as the acidic terminal segment (ATS), while the external domain contains Duffy Binding-like (DBL) domains and Cysteine-rich Inter-Domain Regions (CIDR) that bind to receptors on endothelial cells (Smith *et al.*, 2000, Chen *et al.*, 2000, Avril *et al.*, 2012, Baruch *et al.*, 1996).

Switching expression between different PfEMP1 variants (there are about 60 *var* genes) allows the parasite to undergo antigenic variation, thus evading the host's protective antibody response (Beeson *et al.*, 2001, Scherf *et al.*, 2008, Smith *et al.*, 1995). Thus PfEMP1 is central to both disease pathology and acquisition of immunity (Cham *et al.*, 2009, Chan *et al.*, 2012); however surprisingly little is known about the pathway for export of this protein to the RBC surface.

The classical secretory pathway in eukaryotic cells involves the incorporation of cargo proteins into vesicles for delivery through an endomembrane system to different cellular destinations. Protein trafficking in *P. falciparum*-infected RBCs has an extra level of complexity due to the fact that the parasite resides within a parasitophorous vacuole (PV) inside RBCs. From its intracellular lcoation *P. falciparum* exports proteins that cause extensive modifications to both the RBC cytoplasm and the RBC plasma membrane (Maier *et al.*, 2009). The predicted *P. falciparum* exportome is more extensive and more complex than that of other *Plasmodium* species (Sargeant *et al.*, 2006) and this is thought to underpin its particular virulence.

An intriguing question is how PfEMP1, an integral membrane protein, is trafficked across the parasite plasma and PV membranes, and then delivered correctly to the RBC surface. Mature human RBCs lack the machinery for protein synthesis or trafficking, so the parasite establishes an unusual exomembrane system that extends beyond its own plasma membrane (Goldberg *et al.*, 2010, Hanssen *et al.*, 2010c). Prominent features of this machinery are

organelles known as Maurer's clefts (Lanzer *et al.*, 2006, Bhattacharjee *et al.*, 2008). The term Maurer's cleft is in fact a misnomer, as these are closed cisternal compartments that are thought to act as a sorting compartment for proteins *en route* to the RBC membrane (Tilley *et al.*, 2008). For example PfEMP1 accumulates at the Maurer's clefts before transfer of part of the population to the RBC membrane (Kriek *et al.*, 2003, Waterkeyn *et al.*, 2000).

The machinery for transfer of PfEMP1 across the PV membrane and for delivery to Maurer's clefts has not been characterized. Indeed there is debate about whether proteins are loaded into the Maurer's clefts as they are formed or delivered later (Gruring *et al.*, 2011, Spycher *et al.*, 2006). A recent report suggested that a full complement of Maurer's cleft-like structures is formed soon after invasion of a new host RBC (Gruring *et al.*, 2011). These authors reported that some Maurer's cleft resident proteins are delivered during or soon after Maurer's cleft formation but others are delivered later. This work suggested the existence of a pathway for the trafficking of some proteins, including integral membrane proteins, to pre-formed clefts; however PfEMP1 was not investigated as part of this analysis.

There is also debate about how Maurer's clefts dock onto the RBC membrane, with some studies suggesting specialized tethers (Pachlatko *et al.*, 2010, Hanssen *et al.*, 2008b, Hanssen *et al.*, 2010c) and others suggesting interactions with a meshwork of actin filaments derived from reorganization of the RBC cytoskeleton (Cyrklaff *et al.*, 2011). Moreover it is unclear whether trafficking from the PV membrane to the Maurer's clefts and the RBC membrane is vesicle-mediated or involves cisternal maturation or soluble chaperoned complexes (Lanzer *et al.*, 2006, Gruring *et al.*, 2011, Hanssen *et al.*, 2010c). This work investigates the remodeling processes that establish the exomembrane system and the route for trafficking of PfEMP1 to the RBC surface.

Results

Maurer's clefts are a critical component of the parasite's exomembrane system and an intermediate compartment in the transport of PfEMP1 to the RBC membrane. To investigate the genesis and operation of the parasite's protein export system, we synchronized *P. falciparum* cultures to a 1-2 h window. This enabled us to follow the timing of trafficking of different components using immunofluorescence microscopy and live cell imaging of GFP-chimeras. It was recently reported (Gruring *et al.*, 2011) that a full complement of Maurer's clefts is generated soon after invasion and that additional proteins can be trafficked to pre-formed Maurer's clefts. In agreement with this we found that antibodies recognizing the Maurer's cleft marker, REX1 (Hawthorne *et al.*, 2004), label punctate structures in the RBC cytoplasm from ~2 h post-invasion (Figure 1A,B). The resident Maurer's cleft proteins, Skeleton-Binding Protein-1 (SBP1) (Blisnick *et al.*, 2000) and Membrane-Associated Histidine-Rich Protein-1 (MAHRP1) (Pachlatko *et al.*, 2010), are first detectable at 2 h post-invasion (Figure 1A,B, top panels, aqua arrows). By 6 h post-invasion most of the Maurer's clefts contain detectable levels of all three of these proteins (Figure 1A,B,E).

We examined the timing of delivery of PfEMP1 using an antibody that recognizes the cytoplasmic domain. PfEMP1 is first observed at the parasite surface ~8-11 h post-invasion and adopts a "necklace of beads" pattern (Figure 1C, yellow arrows). This suggests that the PV represents an intermediate compartment in PfEMP1 trafficking. By ~16 h post-invasion, PfEMP1 is present at the Maurer's clefts, where it is co-located with REX1 (Figure 1C, lower panels). This suggests that PfEMP1 is delivered to the Maurer's clefts after the arrival of most of the Maurer's cleft resident proteins. At these later stages some of the PfEMP1 is still present at the parasite surface (Figure 1C, yellow arrows).

We also examined the timing of delivery of Membrane-Associated Histidine-Rich Protein-2 (MAHRP2), a protein associated with tether-like structures implicated in the docking of Maurer's clefts onto the RBC membrane (Pachlatko *et al.*, 2010). We found that MAHRP2-labeled punctate structures are first detected in the RBC cytoplasm as early as 4 h post-invasion and appear to be in close proximity to REX1-labeled structures (Figure 1D). Initially only a sub-set of Maurer's clefts have associated MAHRP2-labeled structures (Figure 1D, aqua arrows and Figure 1E) but by 8 h post-invasion most structures are dual-labeled (Figure 1D, lower panels and Figure 1E).

The above data suggest the orchestrated trafficking of protein components to the Maurer's clefts at different time points. We were interested to determine whether the different Maurer's cleft proteins are mixed in a homogenous fashion upon delivery to the Maurer's clefts or are present in sub-domains. Given the small size of these organelles we studied the locations of different proteins using 3D-Structured Illumination Microscopy (3D-SIM), which provides an 8-fold increase in volume resolution (Hanssen *et al.*, 2010a, Schermelleh *et al.*, 2008) (Figure 2). We used transfectants expressing a REX1-GFP chimera, which has previously been shown to behave in an equivalent manner to endogenous REX1 (Hanssen *et al.*, 2008a, Dixon *et al.*, 2008). 3D-SIM reveals that Maurer's clefts do indeed have protein sub-domains, with REX1-GFP concentrated at the periphery of the organelles and PfEMP1 and MAHRP1 occupying distinct regions within the body of the Maurer's clefts (Figure 2, right hand panels).

We used the REX1-GFP transfectants to examine the organization of Maurer's clefts in live cells (Figure 3A,B). REX1-GFP-labeled structures are observed in the RBC cytoplasm ~4 h post-invasion consistent with native REX1 expression (Figure 3A). These GFP-labeled structures can also be detected by labeling with the membrane marker, BODIPY-ceramide (Figure 3B). We calculate that 14 ± 5 Maurer's clefts are present by ~8 h post-invasion and this number remains constant during further development (Figure 3E). Time-lapse imaging reveals that the REX1-GFP-labeled Maurer's clefts are highly mobile during the early to mid-ring stage of parasite development (Figure S1A, top panel) in agreement with previous reports for MAHRP1-GFP (Spycher *et al.*, 2006) and REX2-GFP (Gruring *et al.*, 2011) transfectants. REX1-GFP-labeled Maurer's clefts become stationary by 22 h post-invasion (Figure S1A, bottom panel).

To examine the potential role of MAHRP2-containing structures, we generated transfectants expressing MAHRP2-GFP under the endogenous promoter (Figure 3C). Fluorescence is observed in punctate structures in the RBC cytoplasm ~4 h post-invasion (Figure 3C), as observed for the native protein (Figure 1D). From 8 – 16 h post-invasion, these structures number 14 ± 5 per cell, then increase to 21 ± 6 at 22 h post-invasion (Figure 3E). Like the Maurer's clefts, the MAHRP2-GFP-structures are initially mobile (Figure S1B, top panel). Co-labeling with BODIPY-ceramide enables visualization of the Maurer's clefts and reveals that the MAHRP2-GFP puncta are closely associated with the BODIPY-ceramide-labeled Maurer's clefts from 8 h post-invasion (Figure 3D). The MAHRP2-GFP puncta and associated Maurer's clefts become stationary at ~22 h post-invasion (Figure S1B, bottom panel). This is consistent with immunofluorescence microscopy of EqtII-permeabilized parasites (~25 h post-invasion) showing that the MAHRP2-labeled structures are closely adjacent to REX1-labeled Maurer's clefts (Figure 3F).

A recent report suggested that Maurer's cleft immobilization involves remodeling of the RBC membrane skeleton to generate branched actin filaments, which are proposed to help immobilize the Maurer's clefts and maintain their architecture (Cyrklaff *et al.*, 2011). It was reported that treatment for 10 min with 1 μM cytochalasin D destroyed the actin filaments that hold the Maurer's clefts in place, leading to an altered Maurer's cleft morphology

(Cyrklaff *et al.*, 2011). To investigate the role of actin remodeling in Maurer's cleft docking we treated ~14 h post-invasion parasites with cytochalasin D. We found that treatment with 1 µM cytochalasin D (even when used for 8 h) did not affect progress of the ring stage parasite into the trophozoite stage (or subsequent division, rupture and reinvasion), and had no effect on the timing or extent of Maurer's cleft immobilization (Figure S2). Treatment of schizont-infected RBCs with 1 µM cytochalasin D completely ablated merozoite invasion (data not shown) as reported previously (Srinivasan *et al.*, 2011), indicating that this concentration is sufficient to affect actin-dependent processes. Treatment of ~14 h post-invasion parasites with a higher concentration of cytochalasin D (10 µM for 8 h) was associated with a substantial loss of parasite viability and was not pursued.

To further investigate the PfEMP1 trafficking process, we have made use of transfectants expressing a mini-PfEMP1-GFP construct (Melcher *et al.*, 2010). This minimal PfEMP1 construct contains the semi-conserved N-terminal region (DBL and CIDR), as well as the transmembrane and C-terminal ATS domains of the R29 var allele, and is expressed from an integrated docking site. The construct, R29var-V5-TM-ATS-GFP, is referred to here as PfEMP1B-GFP. It has previously been shown that part of the population of PfEMP1B-GFP molecules is delivered to the RBC surface, while some remains associated with Maurer's clefts and other intermediate compartments (Melcher *et al.*, 2010). This is similar to the distribution of endogenous PfEMP1 (Figure 1C; (Kriek *et al.*, 2003, Waterkeyn *et al.*, 2000). The availability of the PfEMP1B-GFP transfectants provides the opportunity to image the PfEMP1 trafficking pathway in live cells.

Fluorescence imaging of BODIPY-ceramide co-labeled transfectants reveals that the PfEMP1B-GFP chimera is present at the parasite surface in a "necklace of beads" pattern from ~6 h post-invasion (Figure 4A, B, aqua arrows). In these early stage parasites BODIPY-ceramide-labeled structures (some of which are Maurer's clefts, see Figure 3B) are observed in the RBC cytoplasm but do not contain the PfEMP1B-GFP chimera (Figure 4A-C, white arrows). Between 10-12 h post-invasion PfEMP1B-GFP-containing puncta appear outside the confines of the parasite. Initially these structures are mobile in the RBC cytoplasm (Figure S3A) but by 24 h post-invasion, they appear to have docked at the RBC membrane (Figure S3A). Taken together with the data from Figure 1C, these data show that PfEMP1B-GFP can be trafficked to pre-existing Maurer's cleft structures.

We have used 3D-SIM to further examine the organization of PfEMP1B-GFP at the Maurer's clefts. As for endogenous PfEMP1 (Figure 2B,C), the chimera is observed to associate with interrupted ring or horseshoe-shaped structures (Figure 5A, aqua arrows), with the longest dimension having an average length of ~350 nm. The GFP label partly overlaps with the BODIPY-ceramide signal and additional BODIPY-ceramide-labeled spherical structures with an apparent diameter of ~360 nm were also observed in some cells (Figure 5A, yellow arrows). PfEMP1B-GFP was not associated with these structures and they likely represent tubulovesicular compartments (Elford *et al.*, 1995). As for endogenous PfEMP1 (Figure 2B,C) the chimera appears to occupy sub-domains within the Maurer's clefts that are separate from the domains occupied by REX1 (Figure 5B, right hand panel).

We have used EqtII-permeabilization (Jackson *et al.*, 2007) to introduce antibodies into the RBC cytoplasm. This pre-embedding labeling protocol permits immuno-EM analysis of the PfEMP1B-GFP-containing structures that are accessible from the RBC cytoplasm. Using an antibody recognizing the cytoplasmic domain of PfEMP1 (R3031; (Duffy *et al.*, 2002)), we observed labeling at the Maurer's clefts (Figure 5C) as reported previously (Hanssen *et al.*, 2010a). When EqtII-permeabilized PfEMP1B-GFP transfectants were probed with anti-GFP, a very similar Maurer's cleft labeling profile was observed (Figure 5D-F). As observed by 3D-SIM (Figure 5B), the PfEMP1B-GFP appears to be particularly concentrated on the

body of the Maurer's clefts and somewhat depleted from the ends. In some cells, Maurer's clefts can be seen in very close association with, or tethered to, the RBC or PV membranes (Figure 5D-F).

We employed 3D-SIM to image the PfEMP1B-GFP-containing structures at the parasite surface at enhanced resolution (Figure 6A). The parasite-associated puncta, appear roughly spherical and have an apparent diameter of ~150 nm. We also probed the organization of PfEMP1B-GFP within the different structures in EqtII-treated cells; this procedure leaves the PV membrane largely intact, as judged by the inaccessibility of the PV protein, SERP (Jackson *et al.*, 2007). An anti-GFP antibody recognizes the chimera at the Maurer's clefts but not at the parasite surface (Figure 6B). A similar result was obtained when the samples were probed with an antibody recognizing the cytoplasmic domain of PfEMP1 (Figure S3B). By contrast the C-terminal domain of Exported Protein-1 (Exp1), which faces the RBC cytoplasm (Gunther *et al.*, 1991), is recognized by antibodies against this domain in EqtII-treated cells (Figure S3C). Moreover both populations of the PfEMP1B-GFP chimera are accessible in acetone-fixed smears (data not shown). These data demonstrate that the cytoplasmic domain and the C-terminal GFP fusion are exposed to the RBC cytoplasm in the Maurer's cleft-associated population of PfEMP1B-GFP but are not accessible in the structures at the parasite surface.

We have undertaken immuno-EM in an effort to further characterize the different PfEMP1-containing structures. Post-embedding labeling is challenging in *P. falciparum*-infected RBCs (Hanssen *et al.*, 2010b, Woodcroft *et al.*, 2012), however we achieved labeling in sections of resin-embedded samples. We found gold particles consistently associated with bulging regions of the PV (Figure 6C). There was significantly higher labeling at the PV bulge regions (1 gold per 0.012 μm^2) than in the RBC cytoplasm (1 gold per 2.8 μm^2) and more labeling of the PV bulge regions (5 gold per μm) than of other regions of the PV (0.7 gold per μm). These structures may represent sites where PfEMP1 accumulates before export.

In an effort to further characterize the nature of these compartments, we have undertaken immuno-fluorescence microscopy of the PfEMP1B-GFP transfectants co-labeled with different PV markers. Exp1 is an integral membrane protein associated with the PVM (Kara *et al.*, 1990, Adisa *et al.*, 2003, Gunther *et al.*, 1991). The Exp1 labeling profile appears to be distinct from that of PfEMP1B (Figure 6D). We also examined the location of the PTEX marker, Hsp101 (de Koning-Ward *et al.*, 2009), which is thought to mark sites where PEXEL-containing proteins are exported. The PfEMP1B-containing compartments do not show good overlap with the compartments with which Hsp101 is associated (Figure 6E).

EqtII-permeabilized PfEMP1B-GFP transfectants were labeled with anti-GFP and protein A-gold and prepared for electron tomography (Figure 7). Tilt series were collected from 250 nm sections and used to reconstruct tomograms. Rendering of different features provides a 3D view of the exomembrane system and reveals the cisternal nature of the Maurer's cleft compartments. Protein A-gold-labeled anti-PfEMP1B-GFP is associated with the Maurer's cleft bodies (Figure 7), as previously reported for endogenous PfEMP1 (Hanssen *et al.*, 2008b). Tubular structures with a diameter of ~30 nm are observed in some sections (rendered in gray). These tether-like structures appear to connect the Maurer's cleft bodies to the RBC membrane (Figure 7A,C; Video S1) or the PV membrane (Figure 7F,G; Video S3). In some cases Protein A-gold-labeled anti-PfEMP1B-GFP is associated with these tether-like structures (Figure 7A,C,F,G, Video S1,3).

In this work we have employed an improved algorithm for enhancing the quality of individual tilt projections prior to volumetric reconstruction (Maiorca *et al.*, 2012), as well

as a semi-automatic process for rendering the electron tomograms (see Methods). This reveals additional regions of close association between the RBC membrane and the Maurer's clefts (Figure 7A,B,D, aqua arrows; Video S1,2). These connections may involve extensions of the protein coat underlying the RBC membrane and are reminiscent of recently reported modifications to the RBC cytoskeleton (Cyrklaff *et al.*, 2012). This data is consistent with both tubular tether-like structures and direct RBC cytoskeleton interactions being involved in the attachment of Maurer's clefts to the RBC membrane. In some cases Protein A-gold-labeled anti-PfEMP1B-GFP is associated with these regions of close association (Figure 7B,C).

Our ultrastructural analysis of the PfEMP1-containing structures in the RBC cytoplasm revealed another interesting feature. An antibody recognizing the ATS domain of endogenous PfEMP1 (R3031 (Duffy *et al.*, 2002)) strongly recognized PfEMP1 associated with a population of densely coated ~80 nm vesicles (Figure 8A-C). These are equivalent to the previously described electron-dense vesicles (EDVs) (Hanssen *et al.*, 2010a, Trelka *et al.*, 2000). These vesicles are relatively few in number and are occasionally observed in clumps (Figure 8A), though this clumping could potentially occur during sample preparation. In some cases the EDVs appear to be in the process of fusing with the RBC membrane (Figure 8B,C). Similar structures were labeled with anti-GFP in the PfEMP1B-GFP transfectants (Figure 8D,E, rendered in white). These EDVs sometimes appeared to be in close association with extensions of the RBC membrane (Figure 8E, aqua arrow). Smaller vesicle-like structures (VLS) are also often observed in association with other exomembrane features (rendered in blue). These are not labeled with antibodies recognizing endogenous PfEMP1 or the PfEMP1B-GFP chimera.

Discussion

Recent studies revealed that Maurer's clefts are formed very early after invasion (Gruring *et al.*, 2011). It is likely that an initial suite of proteins is transferred into these organelles as they form, however other resident proteins appear to be delivered in a temporally staggered manner. Here we have confirmed and extended the work of Gruring *et al.* (2011) by showing that REX1 is transferred to Maurer's clefts during or shortly after their genesis (i.e. ~2 h after invasion), while the integral membrane proteins, SBP1 and MAHRP1, are delivered to the Maurer's clefts somewhat later, i.e. after these structures are formed.

In agreement with the work of Gruring *et al.* (2011), we find that the delivery of the later arriving Maurer's cleft proteins is not associated with an increase in Maurer's clefts numbers. This indicates a mechanism for transferring integral membrane proteins to pre-existing Maurer's clefts, and it is interesting to consider how this might occur. We and others have previously reported the presence of two populations of vesicles in the infected RBC cytoplasm. These comprise ~25 nm uncoated VLS (Kriek *et al.*, 2003, Wickert *et al.*, 2003, Hanssen *et al.*, 2008b) and ~80 nm EDVs (Hanssen *et al.*, 2010a, Taraschi *et al.*, 2003, Taraschi *et al.*, 2001). Neither represents an obvious transport vehicle for delivery of proteins to the Maurer's clefts. We have undertaken immuno-labeling experiments using antibodies recognizing SBP1, REX1 and MAHRP1 (Hanssen *et al.*, 2008b, Hanssen *et al.*, 2010a, Hanssen *et al.*, 2008a) and have not observed labeling of the EDVs or VLSs with Maurer's cleft resident proteins. Moreover the ~80 nm EDVs are only observed in trophozoite stage parasites ((Hanssen *et al.*, 2010a) and this study) and thus are not present during Maurer's cleft development. The absence of evidence for a vesicle-mediated pathway supports previous suggestions that these proteins are exported into the RBC cytoplasm as soluble chaperoned complexes, prior to insertion into the Maurer's cleft membrane (Gruring *et al.*, 2011, Knuepfer *et al.*, 2005, Papakrivos *et al.*, 2005). For example structures known as

J-dots that contain parasite-encoded Hsp40 proteins have been suggested to play a role in trafficking of proteins to the Maurer's clefts (Kulzer *et al.*, 2010).

In this work, we used super-resolution microscopy to show that different resident proteins are located in separate regions of the Maurer's clefts. This suggests that the staggered delivery process results in the formation of separate sub-domains. These domains may have distinct functions in the loading and unloading of cargo.

The Maurer's clefts are mobile for the first ~18 h post-invasion and then appear to dock at the RBC membrane. Based on electron tomography data we have previously suggested that the cleft bodies can be connected to the RBC membrane by tubular structures with a distinctive ultrastructural appearance (Hanssen *et al.*, 2008b, Pachlatko *et al.*, 2010). These structures have a diameter of about 30 nm, a length of 200-300 nanometers, and a distinct striated appearance. By contrast, a recent cryoEM analysis of *P. falciparum*-infected RBCs (Cyrklaff *et al.*, 2011) failed to observe these tether-like structures. These authors observed a reorganized RBC membrane skeleton in the region of the Maurer's clefts and instead suggested that the connection between the Maurer's clefts and the RBC membrane involves filamentous actin that is mined from the host cell.

Here we confirm the presence of the tether-like structures in electron tomograms. We further examined the role of tether-like structures in exomembrane architecture by examining the organization and timing of export of a major component of the tethers, MAHRP2 (Pachlatko *et al.*, 2010). MAHRP2 is an essential and completely conserved PEXEL-negative protein, which has no ortholog in any other *Plasmodium* species. It is the only protein known to be uniquely associated with the tubular tether-like structures, and it has been suggested that it may form these structures by inserting into membranes as a monotopic 'hairpin' (Pachlatko *et al.*, 2010). MAHRP2-GFP-labeled punctate structures first appear in the RBC cytoplasm ~4 h after invasion (somewhat earlier than previously appreciated (Pachlatko *et al.*, 2010)) and appear to associate with REX1-labeled Maurer's clefts as mobile complexes. Between 16-22 h post-invasion, the numbers of MAHRP2-GFP-labeled structures increases and the tether/ Maurer's cleft complexes dock onto the RBC membrane. Their physical association and the co-incident immobilization process are consistent with the suggestion that the tethers play a role in the RBC membrane attachment process, however given that the tethers are already attached to the Maurer's clefts prior to immobilization it seems likely that additional events are required to drive the docking of the complex.

We considered the possibility that tether attachment and RBC membrane skeleton remodeling might function together to dock the Maurer's clefts. Indeed there are several reports of close lateral associations of the Maurer's clefts with the RBC membrane (Kriek *et al.*, 2003, Hanssen *et al.*, 2008b, Cooke *et al.*, 2006). In this work we have used non-linear anisotropic diffusion (NAD) filtering to enhance the quality of the reconstructed tomograms. This reveals what appear to be extensions of the protein coat underlying the RBC membrane, linking to the Maurer's clefts. These structures are consistent with a remodeled RBC membrane skeleton as proposed by Cyrklaff *et al.* (2011). Nonetheless, we found that treatment of cultures with 1 μM cytochalasin D for up to 8 h had no effect on the timing of the docking process.

A very recent study, which appeared while this manuscript was under review (Kilian *et al.*, 2012), reported that treatment of trophozoite stage parasites with 10 μM cytochalasin D increased the rate of diffusion of Maurer's clefts in trophozoite stage parasites. We have not examined the effect of treatment with 10 μM cytochalasin D on the initial docking process as an 8 h treatment at this concentration was associated with loss of parasite viability. Thus our results are not directly comparable with the data of Kilian et al. (2012). However it is

interesting to note that these authors found that the rate of diffusion in cytochalasin D-treated trophozoites was still only about one third of the rate observed in ring stage parasites. This may suggest that following destruction of cytoskeletal linkages, attachment by MAHRP2-containing tethers still constrains Maurer's cleft diffusion. Taken together the data are consistent with the suggestion that MAHRP2-containing tethers initiate the docking process and that membrane skeleton remodeling strengthens the interactions and further limits the diffusion rate by providing secondary attachment points.

Of particular interest is the pathway for trafficking of PfEMP1 from the parasite to the Maurer's clefts and from there to the RBC membrane. Transcription of *var* genes is initiated in early ring stage parasites (Kyes *et al.*, 2000), however, PfEMP1 first appears on the infected RBC surface ~16 h post invasion (Gardner *et al.*, 1996). This suggests that export of PfEMP1 across the RBC cytoplasm is a slow process. Some studies provide evidence for the involvement of a chaperoned complex (Knuepfer *et al.*, 2005, Papakrivos *et al.*, 2005), while others suggest that PfEMP1 is transferred to the RBC membrane in transport vesicles (Taraschi *et al.*, 2003, Taraschi *et al.*, 2001, Cyrklaff *et al.*, 2011). Previous efforts to follow the trafficking of GFP-labeled PfEMP1 have used transfectants expressing an unusual KAHRP-PfEMP1 hybrid chimera (Knuepfer *et al.*, 2005). We now have available transgenic parasites expressing constructs that more closely resemble endogenous PfEMP1. PfEMP1B-GFP contains the semi-conserved N-terminal region (DBL, CIDR), as well as the transmembrane and ATS domains and is expressed from an integrated docking site (Melcher *et al.*, 2010). This construct has been shown to be correctly delivered and exposed at the RBC surface.

Using super-resolution optical microscopy we found that PfEMP1B-GFP is first delivered to regions at the parasite surface, where it forms a punctate pattern similar to that observed for endogenous PfEMP1. Selective permeabilization studies showed that the GFP tag is not accessible to antibodies when the chimera is in this location, indicating that the protein is contained within a membrane-bound compartment. EM of samples prepared for post-embedding labeling reveals that the chimera is associated with regions of the parasite surface where the PV membrane bulges into the RBC cytoplasm. The nature and composition of these compartments in not known but structures that may be related were reported in early EM studies (Aikawa *et al.*, 1986, Atkinson *et al.*, 1990). These compartments may be involved in PfEMP1 export, or may represent sites where PfEMP1 accumulates prior to export, or possibly performs an alternative function. The compartments do not show good overlap with the regions of the PV where the PTEX machinery is located, in agreement with another very recent report (Riglar *et al.*, 2013). This may indicate that PfEMP1 is exported by transport machinery that is distinct from the machinery used to export PEXEL-containing proteins. Alternatively PfEMP1 molecules may accumulate in a separate site prior to transfer to the PTEX export site.

Pre-embedding immunoEM labeling confirms that the PV-associated PfEMP1B-GFP population is largely inaccessible to anti-GFP but becomes accessible once it reaches the Maurer's clefts. This confirms that the C-terminal GFP-labeled domain of Maurer's cleft-associated PfEMP1B faces the RBC cytoplasm. Like endogenous PfEMP1 (Hanssen *et al.*, 2010a), PfEMP1B-GFP appears to be concentrated in the central region of the Maurer's cleft bodies.

The mechanism for trafficking of PfEMP1 from the Maurer's clefts to the RBC membrane is of considerable interest. In agreement with previous ultrastructural studies (Trelka *et al.*, 2000, Hanssen *et al.*, 2010c), we observed EDVs at the periphery of RBCs infected with mature parasites. In some sections the vesicles seemed to be in the process of fusing with the RBC membrane, giving rise to cup-shaped electron-dense structures that might be

intermediates in knob structure formation. An antibody that recognizes the cytoplasmic domain of PfEMP1 (Duffy *et al.*, 2002) strongly labels the EDVs in EqtII-permeabilized infected RBCs. Previous post-embedding immuno-labeling studies have revealed PfEMP1 associated with what are likely to be equivalent structures (Trelka *et al.*, 2000, Cyrklaff *et al.*, 2011). Importantly, PfEMP1B-GFP is also associated with EDVs, suggesting that the chimera is following a similar path to endogenous PfEMP1.

We suggest that EDVs are probably not involved in the transport of PfEMP1 from the PV to the Maurer's clefts, as they are only observed in RBCs infected with mature stage parasites (Trelka *et al.*, 2000, Hanssen *et al.*, 2010c). However, the EDVs may be involved in the transport of PfEMP1 from the Maurer's clefts to the RBC membrane. It is interesting to note that antibodies against PfEMP1B-GFP also sometimes recognize the chimera on the tether-like structures. It is also of interest that the timing of immobilization of the tether/Maurer's cleft complexes, the timing of EDV appearance and the timing of delivery of PfEMP1 to the RBC surface (Kriek *et al.*, 2003) are overlapping. While further studies are required to determine the precise mechanism of delivery of PfEMP1 to the RBC surface, it is possible that these structures work together to facilitate the transfer of PfEMP1 from the Maurer's clefts to the RBC membrane.

In conclusion, we have shown that part of the population of PfEMP1 is present in compartments at the PV, which may represent an intermediate destination en route to the Maurer's clefts. We also show that PfEMP1 is associated with EDVs which may play a role in the transfer to the RBC surface. The timing of PfEMP1 delivery to the RBC surface is similar to the timing for Maurer's clefts docking onto the RBC membrane skeleton. This process appears to involve tubular tether-like structure but does not appear to require membrane skeleton reorganization. The availability of transfectants expressing GFP-chimeras of PfEMP1 and components of the exomembrane system will help understand the export process potentially leading to novel ways of combating parasite virulence.

Experimental Procedures

Parasite culture

Parasites were cultured in RPMI-HEPES supplemented with 5% human serum and 0.25% AlbuMAX II (Foley *et al.*, 1994). RBCs and pooled sera were obtained from the Red Cross Transfusion Service (Melbourne, Australia). Parasites were synchronized using two sorbitol treatments (Lambros *et al.*, 1979). Late schizont-stage parasites were harvested using a 65% Percoll cushion, added to pre-cultured RBCs (5% hematocrit) and incubated for 1 or 2 h on a shaker to generate singly-infected rings with a 1 or 2 h age window (Klonis *et al.*, 2011). The excess schizonts were removed by treatment with sorbitol.

Generating transgenic parasites

A MAHRP2-GFP integrant was generated using the pGREP1 plasmid with previously described protocols (Rug *et al.*, 2013). Full length *mahrp2* (excluding the stop codon) was generated by PCR from genomic DNA and cloned into the SacII/XhoI sites on pGREP1 (Forward (5′- GCGCCCGCGG ATGCAGCCTTGTCCATATG - 3′) and reverse primers (5′- CGCGCTCGAG TAATGTTTGTTGTGTACTAGTAGAAG – 3′). This resulted in a full length version of *mahrp2* expressed under the control of the endogenous promoter, with GFP fused at the C-terminus. Parasite transfections were performed as previously described (Wu *et al.*, 1995), and transfectants were cycled three times on/off drug selection to select for integration. REX1-GFP transfectants were generated as described previously (Dixon *et al.*, 2008) and maintained on 50 nM WR99210. PfEMP1B-GFP (R29var-V5-TM-ATS-GFP) transfectants were generated in the IT4 strain as described previously (Melcher *et al.*, 2010).

Immunolabeling

Some immunofluorescence assays were performed on infected RBCs that had been prepared as acetone-fixed smears (Spielmann *et al.*, 2006). Alternatively, #1.5 coverslips (Leica) were treated with 0.125 mg/ml Concanavalin A (Con A) at 37°C for 15 min and washed three times in PBS. Infected RBCs (0.5% haematocrit in phosphate-buffered saline, PBS) were loaded onto the slide, incubated at room temperature for 30 min (in a humidified box) and unbound cells were washed off in PBS. The bound cells were fixed in 2% paraformaldehyde (PFA) (in PBS) for 15 min, washed in PBS and the RBC membrane was selectively permeabilized with ~40 μg/ml Equinatoxin II (EqtII) (Jackson *et al.*, 2007) at room temperature for 10 min. The cells were washed, incubated in 3% Bovine Serum Albumin (BSA) (in PBS) for 30 min, before labeling with primary and secondary antibodies. Samples were incubated with 1 μg/ml DAPI for 10 minutes, washed three times and mounted in 5 mM *p*-phenylenediamine in 10% PBS, pH 8.6, in 90% glycerol, onto #1.5 coverslips (Leica).

Pre-embedding labeling for immuno-EM involved fixing infected RBCs in 2% PFA, permeabilizing with EqtII in suspension (Hanssen *et al.*, 2008b), followed by washing and incubation in 3% BSA (in PBS) for 30 min, before labeling with primary antibodies and gold-labeled protein A (6 nm Aurion). Post-embedding labeling was performed by fixing infected RBCs with 0.5% glutaraldehyde for 30 min on ice, and embedding in LR-White resin as described previously (Hanssen *et al.*, 2010b). Sections (70-90 nm) were cut and labeled with primary antibodies and secondary antibodies conjugated to gold (6 or 10 nm, Aurion).

Primary antibodies were anti-GFP rabbit polyclonal (Humphries *et al.*, 2005) (1:200 or 1:10 for post embedding immuno-EM) or anti-GFP (monoclonal antibodies (MAb), Roche, 1:500), anti-REX1 mouse polyclonal (1:500), anti-REX1 rabbit polyclonal (Hawthorne *et al.*, 2004) (1:500), anti-PfEMP1 ATS (MAb 1B/98-6H1-1, 1:100) (Maier *et al.*, 2007), anti-PfEMP1-ATS rabbit polyclonal ((R3031) (Duffy *et al.*, 2002)) or (Frankland *et al.*, 2007) (1:1000), rabbit anti-MAHRP2 (1:100) (Pachlatko *et al.*, 2010), mouse anti-MAHRP1 (Spycher *et al.*, 2006)), anti-SBP1 (rabbit, 1:2000) (Cooke *et al.*, 2006), anti-Exp1 (mouse 1:100) (Kara *et al.*, 1990) and anti-HSP101 (rabbit, 1:100) (de Koning-Ward *et al.*, 2009). Secondary antibodies were FITC/ Alexa 568/ Alexa 647 anti-rabbit or mouse antibodies (Life Sciences), used at 1:200. For post-embedding immuno-EM labeling, secondary antibodies were gold-conjugated, goat anti-rabbit IgG (H&L, 6 or 10 nm, Aurion), used at 1:20. BODIPY-TR-ceramide labeling was performed as described previously (Adisa *et al.*, 2003).

Fluorescence microscopy

Samples were viewed on a DeltaVision DV Elite™ Restorative Widefield Deconvolution Imaging System (Applied Precision) using a 100x objective (1.4NA). Samples were excited by 390, 475, 542 or 632 nm lasers and imaged using band pass filters at 435, 523, 994 or 676 nm. Immunofluorescence and fixed transfectant data are presented as projections of whole cell z-stacks (taken at intervals of 0.2 μm). For Maurer's cleft and tether number analyses, cells were fixed with 2% PFA/0.005% glutaraldehyde. Live cell imaging of transfectants was performed at 37°C in a closed micro-chamber (iBidi) (Gruring *et al.*, 2012). 3D-Structured Illumination Microscopy (3D-SIM) (Schermelleh et al., 2008) was implemented on a DeltaVision OMX V4 Blaze™ (Applied Precision). Samples were excited using 488, 568 or 642 nm lasers and imaged using band pass filters at 528, 608 and 683 nm with a 60x oil immersion lens (1.42 NA).

All fluorescence images were processed using Image J software (http://rsbweb.nih.gov./ij/). Color, brightness and contrast were modified for clarity. Maurer's cleft and tether numbers are averages of 50 cells ± standard deviation (S.D.) and were quantified using Image J.

Electron microscopy and tomography

Sections (70 nm or 250 nm) were cut, stained with uranyl acetate and lead citrate and observed on a Tecnai G^2 F30 (FEI Company) transmission Electron Microscope (Advanced Microscopy Facility, Bio21 Institute, Melbourne). For electron tomography, tilt series were acquired using the Xplore 3D software (FEI Company). Tomograms were recorded between −66 and +66 degrees at 2° intervals and aligned with IMOD (Kremer *et al.*, 1996, Mastronarde, 1997), as described previously (Abu Bakar *et al.*, 2010, Hanssen *et al.*, 2008b). Where appropriate the data were regularized using pre-NAD filtering (Maiorca *et al.*, 2012) prior to reconstruction using the Filtered Back Projection method. Segmentation and 3D-model rendering employed ITK-SNAP (www.itksnap.org/) and 3dmod (http://bio3d.colorado.edu/). Each model was generated from the reconstructed tomogram using a supervised segmentation approach. Firstly, a user-guided voxel segmentation of the structures of interest was performed using the level set method (Yushkevich *et al.*, 2006). Secondly, the voxel-wise segmented model were imported into 3dmod and manually refined. The final smoothed models were obtained by convolving the volumetric representation of each object in the manually refined model with an isotropic 3D Gaussian of 1 voxel standard deviation (Witkin, 1983, Koenderink, 1984), followed by automatic thresholding (Ostu, 1979).

Supplementary Material

Refer to Web version on PubMed Central for supplementary material.

Acknowledgments

References

Abu Bakar NA, Klonis N, Hanssen E, Chan C, Tilley L. Digestive-vacuole genesis and endocytic processes in the early intraerythrocytic stages of *Plasmodium falciparum*. J Cell Sci. 2010; 123:441–450. [PubMed: 20067995]

Adisa A, Rug M, Klonis N, Foley M, Cowman AF, Tilley L. The signal sequence of exported protein-1 directs the green fluorescent protein to the parasitophorous vacuole of transfected malaria parasites. J Biol Chem. 2003; 278:6532–6542. [PubMed: 12456681]

Aikawa M, Uni Y, Andrutis AT, Howard RJ. Membrane-associated electron-dense material of the asexual stages of *Plasmodium falciparum*: evidence for movement from the intracellular parasite to the erythrocyte membrane. Am J Trop Med Hyg. 1986; 35:30–36. [PubMed: 3511749]

Atkinson CT, Aikawa M. Ultrastructure of malaria-infected erythrocytes. Blood Cells. 1990; 16:351–368. [PubMed: 2257318]

Avril M, Tripathi AK, Brazier AJ, Andisi C, Janes JH, Soma VL, et al. A restricted subset of var genes mediates adherence of *Plasmodium falciparum*-infected erythrocytes to brain endothelial cells. Proc Natl Acad Sci U S A. 2012; 109:E1782–1790. [PubMed: 22619321]

Baruch DI, Gormely JA, Ma C, Howard RJ, Pasloske BL. *Plasmodium falciparum* erythrocyte membrane protein 1 is a parasitized erythrocyte receptor for adherence to CD36, thrombospondin,

and intercellular adhesion molecule 1. Proc Natl Acad Sci U S A. 1996; 93:3497–3502. [PubMed: 8622965]

Baruch DI, Pasloske BL, Singh HB, Bi X, Ma XC, Feldman M, et al. Cloning the *P. falciparum* gene encoding PfEMP1, a malarial variant antigen and adherence receptor on the surface of parasitized human erythrocytes. Cell. 1995; 82:77–87. [PubMed: 7541722]

Beeson JG, Reeder JC, Rogerson SJ, Brown GV. Parasite adhesion and immune evasion in placental malaria. Trends Parasitol. 2001; 17:331–337. [PubMed: 11423376]

Bhattacharjee S, van Ooij C, Balu B, Adams JH, Haldar K. Maurer's clefts of *Plasmodium falciparum* are secretory organelles that concentrate virulence protein reporters for delivery to the host erythrocyte. Blood. 2008; 111:2418–2426. [PubMed: 18057226]

Blisnick T, Morales Betoulle ME, Barale J, Uzureau P, Berry L, Desroses S, et al. Pfsbp1, a Maurer's cleft *Plasmodium falciparum* protein, is associated with the erythrocyte skeleton. Mol. Biochem. Parasitol. 2000; 111:107–121. [PubMed: 11087921]

Carlson J, Helmby H, Hill AV, Brewster D, Greenwood BM, Wahlgren M. Human cerebral malaria: association with erythrocyte rosetting and lack of anti-rosetting antibodies. Lancet. 1990; 336:1457–1460. [PubMed: 1979090]

Cham GK, Turner L, Lusingu J, Vestergaard L, Mmbando BP, Kurtis JD, et al. Sequential, ordered acquisition of antibodies to *Plasmodium falciparum* erythrocyte membrane protein 1 domains. J Immunol. 2009; 183:3356–3363. [PubMed: 19675168]

Chan JA, Howell KB, Reiling L, Ataide R, Mackintosh CL, Fowkes FJ, et al. Targets of antibodies against *Plasmodium falciparum*-infected erythrocytes in malaria immunity. J Clin Invest. 2012; 122:3227–3238. [PubMed: 22850879]

Chen Q, Heddini A, Barragan A, Fernandez V, Pearce SF, Wahlgren M. The semiconserved head structure of *Plasmodium falciparum* erythrocyte membrane protein 1 mediates binding to multiple independent host receptors. J Exp Med. 2000; 192:1–10. [PubMed: 10880521]

Cooke BM, Buckingham DW, Glenister FK, Fernandez KM, Bannister LH, Marti M, et al. A Maurer's cleft-associated protein is essential for expression of the major malaria virulence antigen on the surface of infected red blood cells. J Cell Biol. 2006; 172:899–908. [PubMed: 16520384]

Cyrklaff M, Sanchez CP, Frischknecht F, Lanzer M. Host actin remodeling and protection from malaria by hemoglobinopathies. Trends Parasitol. 2012; 28:479–485. [PubMed: 22980758]

Cyrklaff M, Sanchez CP, Kilian N, Bisseye C, Simpore J, Frischknecht F, Lanzer M. Hemoglobins S and C interfere with actin remodeling in Plasmodium falciparum-infected erythrocytes. Science. 2011; 334:1283–1286. [PubMed: 22075726]

de Koning-Ward TF, Gilson PR, Boddey JA, Rug M, Smith BJ, Papenfuss AT, et al. A newly discovered protein export machine in malaria parasites. Nature. 2009; 459:945–949. [PubMed: 19536257]

Dixon MW, Hawthorne PL, Spielmann T, Anderson KL, Trenholme KR, Gardiner DL. Targeting of the ring exported protein 1 to the Maurer's clefts is mediated by a two-phase process. Traffic. 2008; 9:1316–1326. [PubMed: 18489703]

Dondorp AM, Pongponratn E, White NJ. Reduced microcirculatory flow in severe falciparum malaria: pathophysiology and electron-microscopic pathology. Acta Trop. 2004; 89:309–317. [PubMed: 14744557]

Duffy MF, Brown GV, Basuki W, Krejany EO, Noviyanti R, Cowman AF, Reeder JC. Transcription of multiple var genes by individual, trophozoite-stage *Plasmodium falciparum* cells expressing a chondroitin sulphate A binding phenotype. Molecular microbiology. 2002; 43:1285–1293. [PubMed: 11918813]

Eastman RT, Fidock DA. Artemisinin-based combination therapies: a vital tool in efforts to eliminate malaria. Nat Rev Microbiol. 2009; 7:864–874. [PubMed: 19881520]

Elford BC, Cowan GM, Ferguson DJ. Parasite-regulated membrane transport processes and metabolic control in malaria-infected erythrocytes. Biochem J. 1995; 308:361–374. [PubMed: 7772015]

Fairhurst RM, Bess CD, Krause MA. Abnormal PfEMP1/knob display on Plasmodium falciparum-infected erythrocytes containing hemoglobin variants: fresh insights into malaria pathogenesis and protection. Microbes Infect. 2012; 14:851–862. [PubMed: 22634344]

Foley M, Deady LW, Ng K, Cowman AF, Tilley L. Photoaffinity labeling of chloroquine-binding proteins in *Plasmodium falciparum*. The Journal of biological chemistry. 1994; 269:6955–6961. [PubMed: 8120058]

Frankland S, Elliott SR, Yosaatmadja F, Beeson JG, Rogerson SJ, Adisa A, Tilley L. Serum lipoproteins promote efficient presentation of the malaria virulence protein PfEMP1 at the erythrocyte surface. Eukaryotic cell. 2007; 6:1584–1594. [PubMed: 17644656]

Gardner JP, Pinches RA, Roberts DJ, Newbold CI. Variant antigens and endothelial receptor adhesion in *Plasmodium falciparum*. Proc Natl Acad Sci U S A. 1996; 93:3503–3508. [PubMed: 8622966]

Goldberg DE, Cowman AF. Moving in and renovating: exporting proteins from *Plasmodium* into host erythrocytes. Nat Rev Microbiol. 2010; 8:617–621. [PubMed: 20706280]

Grau GE, Craig AG. Cerebral malaria pathogenesis: revisiting parasite and host contributions. Future Microbiol. 2012; 7:291–302. [PubMed: 22324996]

Gruring C, Heiber A, Kruse F, Ungefehr J, Gilberger TW, Spielmann T. Development and host cell modifications of *Plasmodium falciparum* blood stages in four dimensions. Nat Commun. 2011; 2:165. [PubMed: 21266965]

Gruring C, Spielmann T. Imaging of live malaria blood stage parasites. Methods Enzymol. 2012; 506:81–92. [PubMed: 22341220]

Gunther K, Tummler M, Arnold HH, Ridley R, Goman M, Scaife JG, Lingelbach K. An exported protein of *Plasmodium falciparum* is synthesized as an integral membrane protein. Mol Biochem Parasitol. 1991; 46:149–157. [PubMed: 1852170]

Hansen DS, Schofield L. Natural regulatory T cells in malaria: host or parasite allies? PLoS Pathog. 2010; 6:e1000771. [PubMed: 20442856]

Hanssen E, Carlton P, Deed S, Klonis N, Sedat J, DeRisi J, Tilley L. Whole cell imaging reveals novel modular features of the exomembrane system of the malaria parasite, Plasmodium falciparum. Int J Parasitol. 2010a; 40:123–134. [PubMed: 19766648]

Hanssen E, Goldie KN, Tilley L. Ultrastructure of the asexual blood stages of *Plasmodium falciparum*. Methods Cell Biol. 2010b; 96:93–116. [PubMed: 20869520]

Hanssen E, Hawthorne P, Dixon MW, Trenholme KR, McMillan PJ, Spielmann T, et al. Targeted mutagenesis of the ring-exported protein-1 of Plasmodium falciparum disrupts the architecture of Maurer's cleft organelles. Mol Microbiol. 2008a; 69:938–953. [PubMed: 18573183]

Hanssen E, McMillan PJ, Tilley L. Cellular architecture of *Plasmodium falciparum*-infected erythrocytes. Int J Parasitol. 2010c; 40:1127–1135. [PubMed: 20478310]

Hanssen E, Sougrat R, Frankland S, Deed S, Klonis N, Lippincott-Schwartz J, Tilley L. Electron tomography of the Maurer's cleft organelles of *Plasmodium falciparum*-infected erythrocytes reveals novel structural features. Mol Microbiol. 2008b; 67:703–718. [PubMed: 18067543]

Hawthorne PL, Trenholme KR, Skinner-Adams TS, Spielmann T, Fischer K, Dixon MWA, et al. A novel Plasmodium falciparum ring stage protein, REX, is located in Maurer's clefts. Mol Biochem Parasitol. 2004; 136:181–189. [PubMed: 15481109]

Humphries AD, Streimann IC, Stojanovski D, Johnston AJ, Yano M, Hoogenraad NJ, Ryan MT. Dissection of the mitochondrial import and assembly pathway for human Tom40. J Biol Chem. 2005; 280:11535–11543. [PubMed: 15644312]

Jackson KE, Spielmann T, Hanssen E, Adisa A, Separovic F, Dixon MW, et al. Selective permeabilization of the host cell membrane of *Plasmodium falciparum*-infected red blood cells with streptolysin O and equinatoxin II. The Biochemical journal. 2007; 403:167–175. [PubMed: 17155936]

Kara U, Murray B, Pam C, Lahnstein J, Gould H, Kidson C, Saul A. Chemical characterization of the parasitophorous vacuole membrane antigen QF 116 from *Plasmodium falciparum*. Mol Biochem Parasitol. 1990; 38:19–23. [PubMed: 1690855]

Kilian N, Dittmer M, Cyrklaff M, Ouermi D, Bisseye C, Simpore J, et al. Haemoglobin S and C affect the motion of Maurer's clefts in *Plasmodium falciparum*-infected erythrocytes. Cell Microbiol. 2012

Kim H, Higgins S, Liles WC, Kain KC. Endothelial activation and dysregulation in malaria: a potential target for novel therapeutics. Curr Opin Hematol. 2011; 18:177–185. [PubMed: 21423010]

Klonis N, Crespo-Ortiz MP, Bottova I, Abu-Bakar N, Kenny S, Rosenthal PJ, Tilley L. Artemisinin activity against *Plasmodium falciparum* requires hemoglobin uptake and digestion. Proc Natl Acad Sci U S A. 2011; 108:11405–11410. [PubMed: 21709259]

Knuepfer E, Rug M, Klonis N, Tilley L, Cowman AF. Trafficking of the major virulence factor to the surface of transfected *P. falciparum*-infected erythrocytes. Blood. 2005; 105:4078–4087. [PubMed: 15692070]

Koenderink J. The structure of images. Biological Cybernetics. 1984; 50:363–370. [PubMed: 6477978]

Kremer JR, Mastronarde DN, McIntosh JR. Computer visualization of three-dimensional image data using IMOD. J Struct Biol. 1996; 116:71–76. [PubMed: 8742726]

Kriek N, Tilley L, Horrocks P, Pinches R, Elford BC, Ferguson DJ, et al. Characterization of the pathway for transport of the cytoadherence-mediating protein, PfEMP1, to the host cell surface in malaria parasite-infected erythrocytes. Mol Microbiol. 2003; 50:1215–1227. [PubMed: 14622410]

Kulzer S, Rug M, Brinkmann K, Cannon P, Cowman A, Lingelbach K, et al. Parasite-encoded Hsp40 proteins define novel mobile structures in the cytosol of the *P. falciparum*-infected erythrocyte. Cell Microbiol. 2010; 12:1398–1420. [PubMed: 20482550]

Lambros C, Vanderberg JP. Synchronization of *Plasmodium falciparum* erythrocytic stages in culture. J Parasitol. 1979; 65:418–420. [PubMed: 383936]

Langreth SG, Peterson E. Pathogenicity, stability, and immunogenicity of a knobless clone of *Plasmodium falciparum* in Colombian owl monkeys. Infect Immun. 1985; 47:760–766. [PubMed: 3882566]

Lanzer M, Wickert H, Krohne G, Vincensini L, Braun Breton C. Maurer's clefts: a novel multi-functional organelle in the cytoplasm of *Plasmodium falciparum*-infected erythrocytes. International journal for parasitology. 2006; 36:23–36. [PubMed: 16337634]

Maier AG, Cooke BM, Cowman AF, Tilley L. Malaria parasite proteins that remodel the host erythrocyte. Nat Rev Microbiol. 2009; 7:341–354. [PubMed: 19369950]

Maier AG, Rug M, O'Neill M,T, Beeson JG, Marti M, Reeder J, Cowman AF. Skeleton-binding protein 1 functions at the parasitophorous vacuole membrane to traffic PfEMP1 to the *Plasmodium falciparum*-infected erythrocyte surface. Blood. 2007; 109:1289–1297. [PubMed: 17023587]

Maiorca M, Hanssen E, Kazmierczak E, Maco B, Kudryashev M, Hall R, et al. Improving the quality of electron tomography image volumes using pre-reconstruction filtering. J Struct Biol. 2012; 180:132–142. [PubMed: 22683346]

Mastronarde DN. Dual-axis tomography: an approach with alignment methods that preserve resolution. J Struct Biol. 1997; 120:343–352. [PubMed: 9441937]

McPherson GG, Warrell MJ, White NJ, Looareesuwan S, Warrel DA. Human cerebral malaria. A quantitative ultrastructural analysis of parasitized erythrocyte sequestration. Am J Pathol. 1985; 119:385–401. [PubMed: 3893148]

Melcher M, Muhle RA, Henrich PP, Kraemer SM, Avril M, Vigan-Womas I, et al. Identification of a role for the PfEMP1 semi-conserved head structure in protein trafficking to the surface of *Plasmodium falciparum* infected red blood cells. Cell Microbiol. 2010; 12:1446–1462. [PubMed: 20438573]

Murray CJL, Rosenfeld LC, Lim SS, Andrews KG, Foreman KJ, Haring D, et al. Global malaria mortality between 1980 and 2010: a systematic analysis. The Lancet. 2012; 379:413–431.

Okiro EA, Bitira D, Mbabazi G, Mpimbaza A, Alegana VA, Talisuna AO, Snow RW. Increasing malaria hospital admissions in Uganda between 1999 and 2009. BMC Med. 2011; 9:37. [PubMed: 21486498]

Ostu N. A threshold selection method from gray-level histogram. IEEE Transactions on Systems, Man and Cybernetics. 1979; 9:62–66.

Pachlatko E, Rusch S, Muller A, Hemphill A, Tilley L, Hanssen E, Beck HP. MAHRP2, an exported protein of *Plasmodium falciparum*, is an essential component of Maurer's cleft tethers. Molecular Microbiology. 2010; 77:1136–1152. [PubMed: 20624222]

Papakrivos J, Newbold CI, Lingelbach K. A potential novel mechanism for the insertion of a membrane protein revealed by a biochemical analysis of the Plasmodium falciparum cytoadherence molecule PfEMP-1. Mol Microbiol. 2005; 55:1272–1284. [PubMed: 15686570]

Planche T, Krishna S. Severe malaria: metabolic complications. Curr Mol Med. 2006; 6:141–153. [PubMed: 16515507]

Riglar DT, Rogers KL, Hanssen E, Turnbull L, Bullen HE, Charnaud SC, et al. Spatial association with PTEX complexes defines regions for effector export into *Plasmodium falciparum*-infected erythrocytes. Nat Commun. 2013; 4:1415. [PubMed: 23361006]

Roberts DJ, Craig AG, Berendt AR, Pinches R, Nash G, Marsh K, Newbold CI. Rapid switching to multiple antigenic and adhesive phenotypes in malaria. Nature. 1992; 357:689–692. [PubMed: 1614515]

Rowe JA, Claessens A, Corrigan RA, Arman M. Adhesion of *Plasmodium falciparum*-infected erythrocytes to human cells: molecular mechanisms and therapeutic implications. Expert Rev Mol Med. 2009; 11:e16. [PubMed: 19467172]

Rug M, Maier AG. Transfection of Plasmodium falciparum. Methods Mol Biol. 2013; 923:75–98. [PubMed: 22990772]

Sargeant TJ, Marti M, Caler E, Carlton JM, Simpson K, Speed TP, Cowman AF. Lineage-specific expansion of proteins exported to erythrocytes in malaria parasites. Genome Biol. 2006; 7:R12. [PubMed: 16507167]

Scherf A, Lopez-Rubio JJ, Riviere L. Antigenic variation in *Plasmodium falciparum*. Annu Rev Microbiol. 2008; 62:445–470. [PubMed: 18785843]

Schermelleh L, Carlton PM, Haase S, Shao L, Winoto L, Kner P, et al. Subdiffraction multicolor imaging of the nuclear periphery with 3D structured illumination microscopy. Science. 2008; 320:1332–1336. [PubMed: 18535242]

Smith JD, Chitnis CE, Craig AG, Roberts DJ, Hudson-Taylor DE, Peterson DS, et al. Switches in expression of Plasmodium falciparum var genes correlate with changes in antigenic and cytoadherent phenotypes of infected erythrocytes. Cell. 1995; 82:101–110. [PubMed: 7606775]

Smith JD, Craig AG, Kriek N, Hudson-Taylor D, Kyes S, Fagan T, et al. Identification of a *Plasmodium falciparum* intercellular adhesion molecule-1 binding domain: a parasite adhesion trait implicated in cerebral malaria. Proc Natl Acad Sci U S A. 2000; 97:1766–1771. [PubMed: 10677532]

Spielmann T, Hawthorne PL, Dixon MW, Hannemann M, Klotz K, Kemp DJ, et al. A cluster of ring stage-specific genes linked to a locus implicated in cytoadherence in Plasmodium falciparum codes for PEXEL-negative and PEXEL-positive proteins exported into the host cell. Mol Biol Cell. 2006; 17:3613–3624. [PubMed: 16760427]

Spycher C, Rug M, Klonis N, Ferguson DJ, Cowman AF, Beck HP, Tilley L. Genesis of and trafficking to the Maurer's clefts of Plasmodium falciparum-infected erythrocytes. Mol Cell Biol. 2006; 26:4074–4085. [PubMed: 16705161]

Srinivasan P, Beatty WL, Diouf A, Herrera R, Ambroggio X, Moch JK, et al. Binding of Plasmodium merozoite proteins RON2 and AMA1 triggers commitment to invasion. Proc Natl Acad Sci U S A. 2011; 108:13275–13280. [PubMed: 21788485]

Taraschi TF, O'Donnell ME, Martinez S, Schneider T, Trelka D, Fowler VM, et al. Generation of an erythrocyte vesicle transport system by *Plasmodium falciparum* malaria parasites. Blood. 2003; 102:3420–3426. [PubMed: 12869498]

Taraschi TF, Trelka D, Martinez S, Schneider T, O'Donnell ME. Vesicle-mediated trafficking of parasite proteins to the host cell cytosol and erythrocyte surface membrane in *Plasmodium falciparum* infected erythrocytes. Int J Parasitol. 2001; 31:1381–1391. [PubMed: 11566305]

Tilley L, Sougrat R, Lithgow T, Hanssen E. The twists and turns of Maurer's cleft trafficking in P. falciparum-infected erythrocytes. Traffic. 2008; 9:187–197. [PubMed: 18088325]

Trelka DP, Schneider TG, Reeder JC, Taraschi TF. Evidence for vesicle-mediated trafficking of parasite proteins to the host cell cytosol and erythrocyte surface membrane in *Plasmodium falciparum* infected erythrocytes. Mol Biochem Parasitol. 2000; 106:131–145. [PubMed: 10743617]

Turner GD, Morrison H, Jones M, Davis TM, Looareesuwan S, Buley ID, et al. An immunohistochemical study of the pathology of fatal malaria. Evidence for widespread endothelial activation and a potential role for intercellular adhesion molecule-1 in cerebral sequestration. Am J Pathol. 1994; 145:1057–1069. [PubMed: 7526692]

Waterkeyn JG, Wickham ME, Davern KM, Cooke BM, Coppel RL, Reeder JC, et al. Targeted mutagenesis of *Plasmodium falciparum* erythrocyte membrane protein 3 (PfEMP3) disrupts cytoadherence of malaria-infected red blood cells. EMBO J. 2000; 19:2813–2823. [PubMed: 10856227]

Wickert H, Wissing F, Andrews KT, Stich A, Krohne G, Lanzer M. Evidence for trafficking of PfEMP1 to the surface of *P. falciparum*-infected erythrocytes via a complex membrane network. Eur J Cell Biol. 2003; 82:271–284. [PubMed: 12868595]

Witkin, A. Scale-space filtering; Proceedings of the 8th International Joint Conference on Artificial Intelligence; Karlsruhe, Germany. 1983; p. 1019-1021.

Woodcroft BJ, McMillan PJ, Dekiwadia C, Tilley L, Ralph SA. Determination of protein subcellular localization in apicomplexan parasites. Trends Parasitol. 2012

World_Health_Organisation. World Malaria Report 2011. 2011. World Malaria Report 2011

Wu Y, Sifri CD, Lei HH, Su XZ, Wellems TE. Transfection of Plasmodium falciparum within human red blood cells. Proc Natl Acad Sci U S A. 1995; 92:973–977. [PubMed: 7862676]

Yushkevich PA, Piven J, Hazlett HC, Smith RG, Ho S, Gee JC, Gerig G. User-guided 3D active contour segmentation of anatomical structures: Significantly improved efficiency and reliability. Neuroimage. 2006; 31:1116–1128. [PubMed: 16545965]
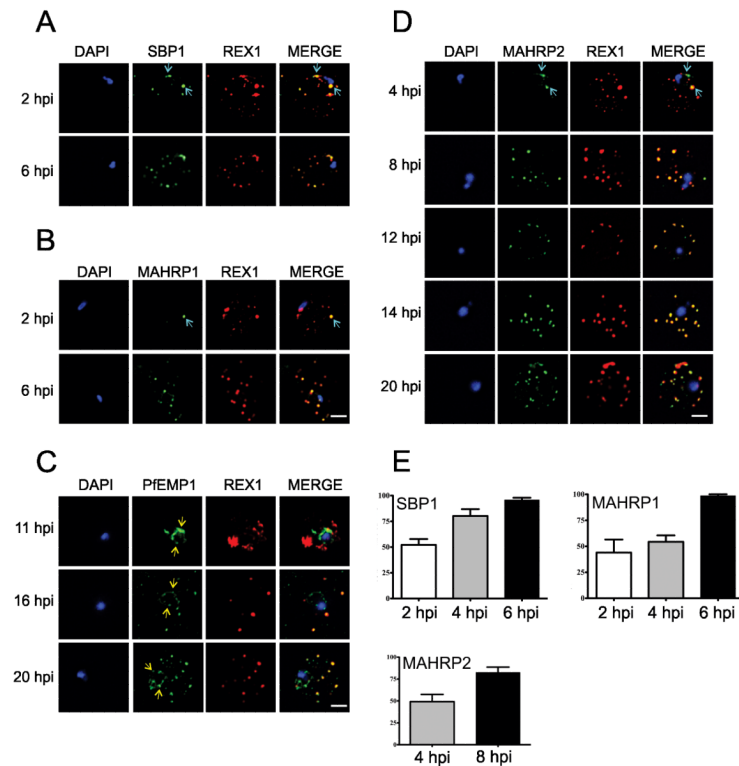
Figure 1. Immunofluorescence microscopy showing staggered delivery of different exomembrane components

(A-D) Infected RBCs were synchronized to a 1 h window, samples were collected at 2 h intervals and smears were fixed with acetone and stained with antibodies recognizing REX1, MAHRP1, SBP1, MAHRP2 and PfEMP1 (ATS) and co-stained with DAPI. Images are presented at time points before and after delivery to the RBC cytoplasm. Scale bars = 3 μm. (E) Mean percentages ± S.E. of Maurer's clefts (as determined by REX1 labeling) that have detectable levels of SBP1, MAHRP1 and MAHRP2. (Based on analysis of 5-10 cells).
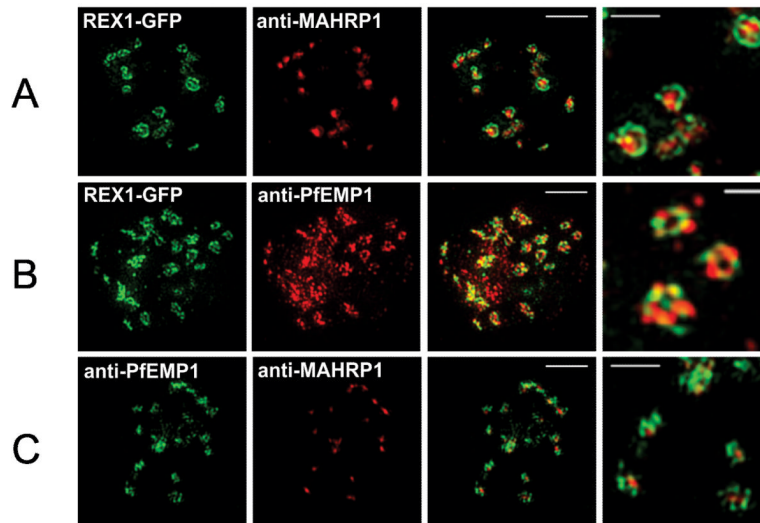
Figure 2. 3D-SIM analysis of the organization of Maurer's cleft resident proteins
REX1-GFP transfectants were permeabilized with EqtII and labeled with antibodies recognizing GFP, PfEMP1 (ATS) or MAHRP1 and 3D stacks were generated by 3D-SIM. Higher magnification images at right. Scale bars = 2 µm, first 3 columns; 500 nm, last column.
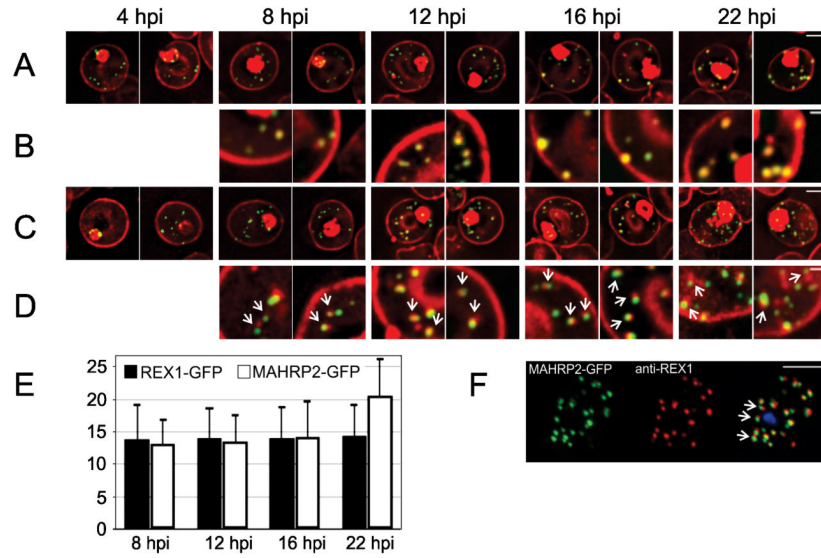
Figure 3. Live cell time course showing assembly of exomembrane components
Transfectants expressing GFP chimeras of (A, B) REX1 and (C, D) MAHRP2 were co-labeled with BODIPY-ceramide. Infected RBCs were synchronized to a ~2 h window and samples were collected at 4 h intervals. BODIPY-ceramide- and REX1-GFP-labeled Maurer's clefts and MAHRP2-GFP-labled structures are evident in the RBC cytoplasm from ~4 h post invasion. MAHRP2-GFP-labled structures are associated with the BODIPY-ceramide-labeled Maurer's clefts (D, white arrows). (E) Quantitative analysis of the number of REX-GFP and MAHRP2-GFP labeled structures in the RBC cytoplasm at different time points. (F) MAHRP2-GFP transfectants were permeabilized with EqtII and labeled with antibodies recognizing REX1. Scale bars = 3 µm (A, C), 1 µm (B, D) and 4 µm (F). See Figure S1, S2 for time series.
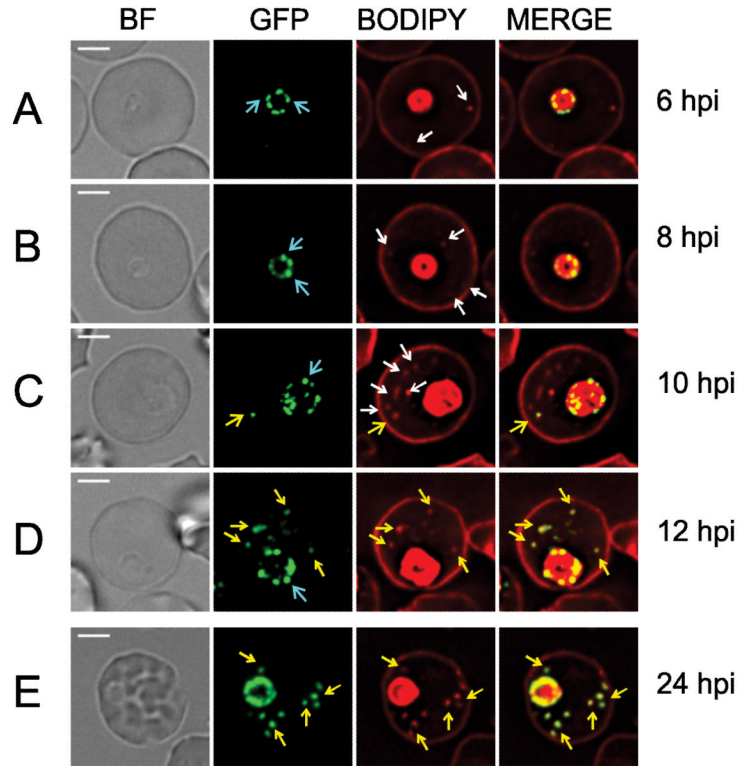
Figure 4. Live cell imaging showing intermediate compartments and timing of export of PfEMP1B-GFP

PfEMP1B-GFP transfectants were co-labeled with BODIPY-ceramide and samples were collected from a tightly synchronized culture (2 hours). (A) BODIPY-ceramide-labeled features (white arrows) are present in the RBC cytoplasm by 6 h post-invasion, while PfEMP1B-GFP is still located in a "necklace of beads" pattern at the parasite surface (aqua arrows). (C) At 10-12 h post-invasion PfEMP1B-GFP is observed in compartments in the RBC cytoplasm (yellow arrows). (E) By ~24 h post-invasion the PfEMP1B-GFP-labeled structures have become immobilized (see Figure S3 for time series). Scale bars = 3 μm.
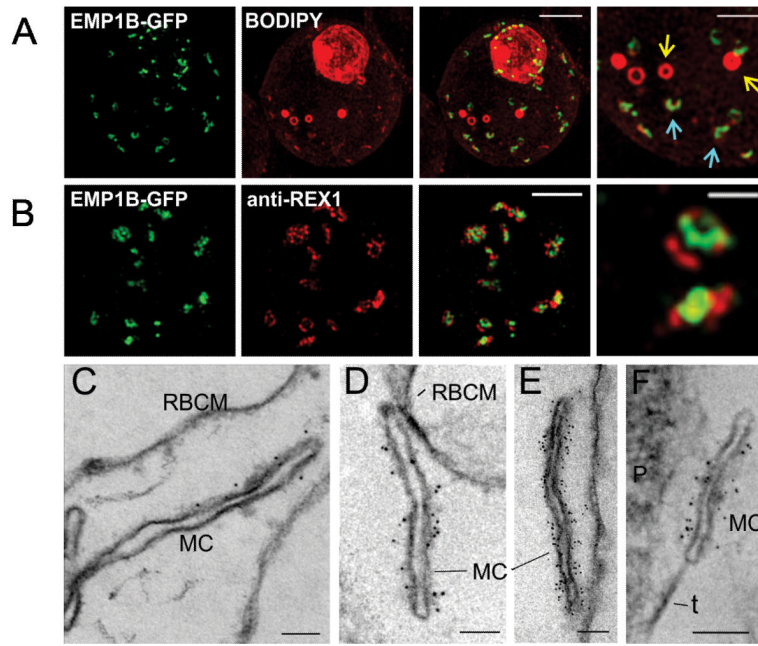
Figure 5. Characterization of PfEMP1B-GFP at Maurer's clefts
(A) Transfectants (ITK strain) expressing the PfEMP1B-GFP chimera were co-labeled with BODIPY-ceramide and imaged using 3D-SIM. Higher magnification images are displayed in the right column. PfEMP1B-GFP is present in horseshoe-shaped Maurer's clefts (aqua arrows). Spherical structures with no GFP labeling are marked with yellow arrows. (B) EqtII-permeabilized PfEMP1B-GFP transfectants were probed with antibodies recognizing GFP and REX1 and imaged by 3D-SIM. (C-F) EqtII-permeabilized 3D7 strain or PfEMP1B-GFP transfectants were labeled with anti-PfEMP1 ATS (C) or anti-GFP (D-F) and 6 nm Protein A-gold, and prepared for EM. A tether (t) and the parasite (P) are indicated. Scale bars = 2 µm (A, first three columns, B), 1 µm (A, last column), 500 nm (B, last column), 100 nm (C-F).
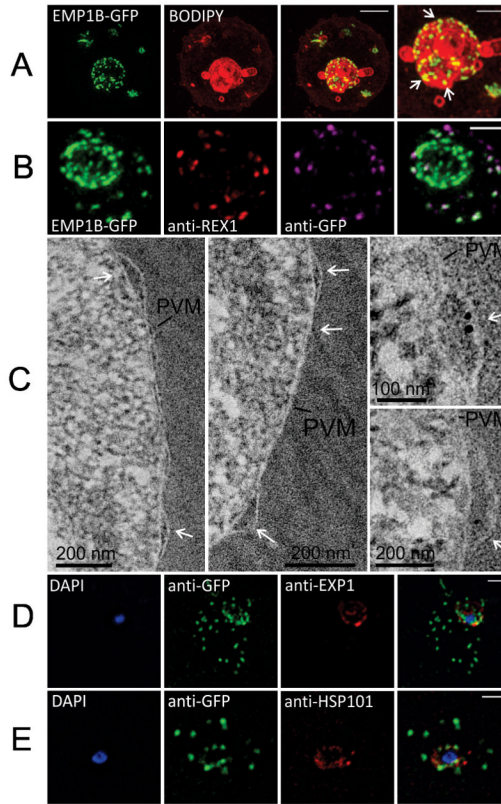
Figure 6. Characterization of an intermediate compartment in PfEMP1 export
(A) Transfectants (ITK strain) expressing the PfEMP1B-GFP chimera were co-labeled with BODIPY-ceramide and imaged using 3D-SIM. See higher magnification image at right. (B) PfEMP1B-GFP transfectants (endogenous GFP fluorescence; green) were permeabilized with EqtII and antibody-accessible epitopes were labeled with anti-GFP (magenta) and anti-REX1 (red). (C) PfEMP1B-GFP transfectants were fixed and resin-embedded and sections were labeled with anti-GFP and protein-A-gold (6 nm left panels, 10 nm right panels). Labeling is observed at bulges in the PV (arrows). (D) Smears of PfEMP1B-GFP transfectant-infected RBCs were fixed with acetone: methanol and stained with antibodies recognizing GFP and Exp1 (D) or Hsp101 (E). Scale bars = 2 µm (A, first three columns), 1 µm (A, last column), 2 µm (B), as marked (C) and 2 µm (D, E).
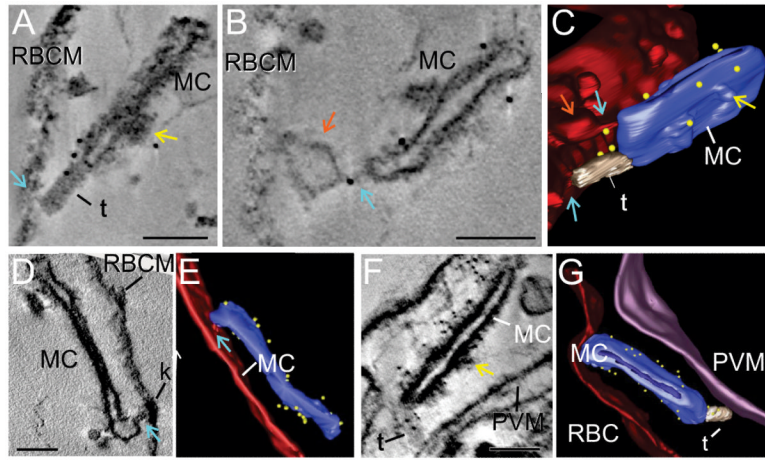
Figure 7. Immuno-electron tomography of Maurer's cleft-associated PfEMP1
EqtII-permeabilized PfEMP1B-GFP transfectants were labeled with antibodies recognizing GFP and prepared for electron tomography. Virtual sections (thickness: 24 nm A,B; 1.2 nm D; 1.5 nm F) from the tomograms and rendered models are presented. (A-C) A tether-like structure (t) connects a Maurer's cleft (MC) to the RBC membrane. (D, E) Region where the Maurer's cleft is closely opposed to the RBC membrane. (F, G) A tether-like structure (t) connects the Maurer's cleft (MC) to the PV membrane. The RBC membrane is rendered in red, the Maurer's clefts in blue, tethers in gray, the PV membrane in purple, and gold particles in yellow. A bulge in the RBC membrane is indicated with orange arrows. Regions that may represent RBC cytoskeleton extensions are indicated with aqua arrows. Thickening of the Maurer's cleft coat is observed in some regions and is indicated with yellow arrows. Scale bars = 100 nm. See Videos S1-S3 for rotations of the models.
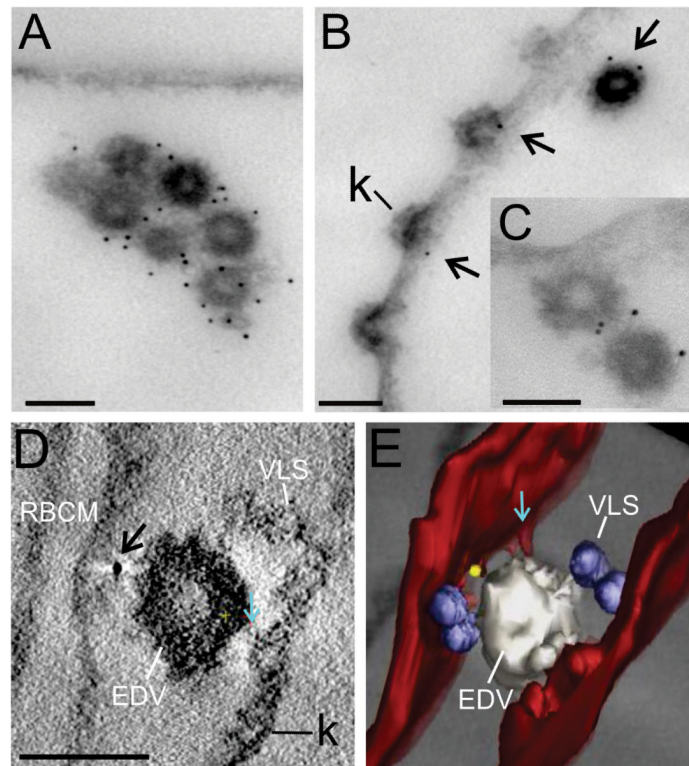
Figure 8. Immuno-EM of EDVs with associated PfEMP1
EqtII-permeabilized 3D7 strain parasites (A-C) and PfEMP1B-GFP transfectants (ITK strain) (D, E) were labeled with antibodies recognizing the ATS (A-C) or GFP (D, E) and prepared for EM (A-C) or tomography (D, E). Arrows indicate gold particles. The RBC membrane is rendered in red, VLS in blue, EDV in white and a gold particle in yellow. A region that may represent an RBC cytoskeleton extension is indicated with aqua arrows. Scale bar = 100 nm.